Analytic study of the three-urn model for separation of sand

G. M. Shim, B. Y. Park, J. D. Noh, and Hoyun Lee
Department of Physics, Chungnam National University, Daejeon 305-764, Korea
(Received 6 February 2004; published 27 September 2004)

We present an analytic study of the three-urn model for separation of sand, which can be regarded as a zero-range process. We solve analytically the master equation and the first-passage problem. We find that the stationary probability distribution obeys the detailed balance and is governed by the free energy. We find that the characteristic lifetime of a cluster diverges algebraically with exponent $1/3$ at the limit of stability. We also give a general argument that the scaling behavior is robust with respect to different expressions of the flux.

DOI: 10.1103/PhysRevE.70.031305 PACS number(s): 45.70.−n, 68.35.Rh

I. INTRODUCTION

A granular system consisting of macroscopic particles exhibits extremely rich phenomena, which have been studied both experimentally and theoretically [1]. One such interesting phenomenon is the spatial separation of shaken sand. In the experiment by Schlichting and Nordmeier [2], granular particles are prepared in a box which is mounted on a shaker and separated into two equal parts by a wall. There is a slit on the wall through which particles can move from one compartment to the other. Under a certain shaking condition, the granular particles simultaneously separate into dense and dilute regions, which will not occur for gaseous particles, due to the dissipative nature of macroscopic particle collisions.

The emergence of symmetry breaking in shaken sand was first explained by Eggers using a hydrodynamic approach [3], and later by Lipowski and Droz using an urn model, which is supposed to capture the essence of the experimental system [4]. In the urn model, N granular particles are distributed into L urns. Each particle can jump from one urn to another with a probability controlled by a parameter, called the effective temperature, which depends explicitly on the density of particles in each urn. The dissipative nature of the particle collision is incorporated into the model using the density-dependent effective temperature.

The model may be regarded as a zero-range process, which was first defined by Spitzer [5], and has been studied extensively recently [6–8]. A zero-range process refers to a dynamic process for particles on an arbitrary lattice where particle hopping rates depend only on the number of particles at departure sites. The results of the zero-range process allow for the formal description of the steady state of the model for fixed N, which could be used in getting the stationary probability distribution in the thermodynamic limit.

The urn model is simple enough to allow extensive numerical calculations [4,9] as well as analytical studies [10,11]. The two-urn ($L=2$) model shows a rich structure with symmetric, mixed, and asymmetric phases separated by continuous and discontinuous transitions, as well as a tricritical point. In the symmetric phase particles are distributed equally in each urn, while the symmetry is broken in the asymmetric phase. In the mixed phase, both the symmetric and asymmetric states are stable. It was also found that the characteristic time that it takes to reach the symmetric state from an asymmetric state is given by the same free energy function that governs the stationary probability distribution [10]. Coppex *et al.* also numerically investigated the three-urn model and found the absence of a continuous transition [9]. They also obtained that the characteristic time at the limit of stability diverges algebraically as the number of particles increases (see also Ref. [12]).

In this paper, we present the results of an analytic study of the master equation and the characteristic time scale in the three-urn model. We solve the master equation in the thermodynamic limit to find that the solution shows the nature of a deformed wave. We also obtain the stationary probability distribution in a finite system, which, interestingly, obeys detailed balance. By combining the knowledge of the characteristic scales of those distributions and the mean-field flux equation, we obtain the scaling property of the characteristic time scale at the limit of stability. We also discuss the robustness of the scaling behavior with respect to different expressions of the flux.

The paper is organized as follows. In Sec. II we briefly review the model and its master equation. In Sec. III we present the analytic solution of the master equation in the thermodynamic limit and the analytic expression of the stationary probability distribution. In Sec. IV we investigate the scaling law of the characteristic time scale. Section V is devoted to conclusions and discussions.

II. THE MODEL AND ITS MASTER EQUATION

The model introduced by Coppex *et al.* [9] is defined as follows. N particles are distributed between three urns, and the number of particles in each urn is denoted as N_1, N_2, and $N_3 = N - N_1 - N_2$, respectively. At each time of update one of the N particles is randomly chosen. Let n be a fraction of the total number of particles in the urn which the selected particle belongs to. With probability $\exp[-1/T(n)]$ the selected particle moves to a randomly chosen neighboring urn. $T(n) = T_0 + \Delta(1-n)$ is the effective temperature of an urn with particles nN, which measures the strength of fluctuations in the urn. For a more detailed description of the model, we refer readers to Ref. [4].

It is easy to derive the master equation for the probability distribution $p(N_1, N_2, N_3, t)$ that there are N_i particles in urn i at time t,

$$p(N_1,N_2,N_3,t+1) = F\left(\frac{N_1+1}{N}\right)\tfrac{1}{2}[p(N_1+1,N_2-1,N_3,t) + p(N_1+1,N_2,N_3-1,t)] + F\left(\frac{N_2+1}{N}\right)\tfrac{1}{2}[p(N_1-1,N_2+1,N_3,t) + p(N_1,N_2+1,N_3-1,t)] + F\left(\frac{N_3+1}{N}\right)\tfrac{1}{2}[p(N_1-1,N_2,N_3+1,t) + p(N_1,N_2-1,N_3+1,t)] + \left[1-\sum_{i=1}^{3}F\left(\frac{N_i}{N}\right)\right]p(N_1,N_2,N_3,t), \quad (1)$$

where $F(n)=n\exp[-1/T(n)]$ measures the flux of particles leaving the given urn. Here we introduced for convenience the notation $p(N_1,N_2,N_3,t)=0$ if $N_1+N_2+N_3\neq N$ or any N_i is either less than 0 or greater than N.

Let us denote the occupancies of the urns by $n_i=N_i/N$. The time evolution of the averaged particle occupancies is governed by the equations

$$\langle n_i\rangle_{t+1} = \langle n_i\rangle_t + \frac{1}{N}\langle \mathcal{F}_i(\vec{n})\rangle_t, \quad (2)$$

where $\langle\cdots\rangle_t=\Sigma_{N_1,N_2,N_3}(\cdots)p(N_1,N_2,N_3,t)$, and $\mathcal{F}_i(\vec{n}) = \frac{1}{2}\Sigma_{k=1}^{3}F(n_k)-\frac{3}{2}F(n_i)$. The unit of time may be chosen such that there is a single update per particle on average. Scaling the time by N, expanding Eq. (2) with respect to $1/N$, and using the mean-field approximation in evaluating the average, we get

$$\frac{d}{dt}n_i(t) = \mathcal{F}_i(\vec{n}(t)), \quad (3)$$

where $n_i(t)=\langle n_i\rangle_t$.

Detailed analysis of the existence of the stable stationary solutions of Eq. (3) was done by Coppex *et al.* [9]. We here display their phase diagram in Fig. 1 to make our paper as self-contained as possible. The stable symmetric solution $(n_1=n_2=n_3)$ exists in regions I, III, and IV while the stable asymmetric solution $(n_1>n_2=n_3)$ exists in regions II, III, and IV. Note that Eq. (3) is obtained with the mean-field approximation that $\langle\mathcal{F}(\vec{n})\rangle=\mathcal{F}(\langle\vec{n}\rangle)$. However, as will be shown later, the relation becomes exact for the δ-function-peaked initial probability distribution, as does the phase diagram.

III. THE SOLUTION OF THE MASTER EQUATION

We are mainly interested in investigating the properties of the infinite system. Consider the thermodynamic limit $N\to\infty$ with the occupancies of the urns n_i being fixed. Representing the probability distribution by n_i instead of N_i, scaling the time by N, expanding Eq. (1) with respect to $1/N$, and keeping the terms up to first order, we arrive at the partial differential equation

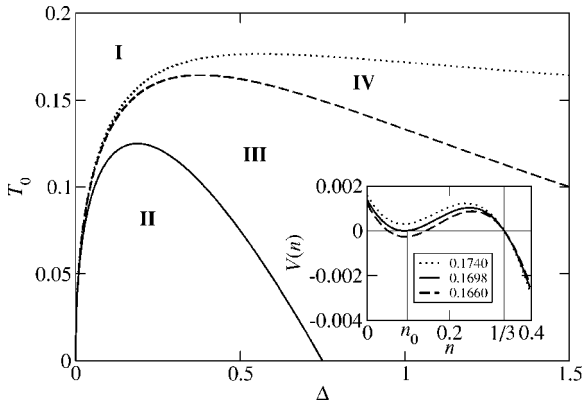

FIG. 1. Phase diagram of the three-urn model [9]. The symmetric solution vanishes continuously on the solid line while the asymmetric one disappears discontinuously on the dotted line. The transition of the behavior of the stationary probability distribution is denoted by the dashed line. For the inset, see Sec. IV.

$$\frac{\partial}{\partial t}p(\vec{n},t) + \frac{\partial}{\partial n_1}[\mathcal{F}_1(\vec{n})p(\vec{n},t)] + \frac{\partial}{\partial n_2}[\mathcal{F}_2(\vec{n})p(\vec{n},t)] = 0. \quad (4)$$

Here we would like to recall that $n_3=1-n_1-n_2$ so that the independent variables are n_1,n_2.

Note that Eq. (4) may be interpreted as the continuity equation for the probability with velocity $(\mathcal{F}_1,\mathcal{F}_2)$. Since the velocity is already given as a function of $\vec{n}$, the solution to Eq. (4) can be formally found as follows. The time evolution of a point located at $\vec{r}=(x,y,1-x-y)$ at $t=0$ is determined by Eq. (3). We denote it by $\vec{R}(t;\vec{r})$. We show its typical trajectories in Fig. 2. In the symmetric phase (region I in Fig. 1) there is only the stable fixed point corresponding to the symmetric state so that every trajectory flows to that point. This is shown in Fig. 2(a). Figure 2(b) shows a typical behavior for the asymmetric phase (region II in Fig. 1). In this case, there are three stable fixed points corresponding to asymmetric states and one unstable fixed point corresponding to the symmetric state as well as three saddle points. The trajectories are separated by the separatrices denoted by dashed lines. Finally, Fig. 2(c) shows a typical behavior for the mixed phase (regions III and IV in Fig. 1). There are one stable symmetric fixed point and three asymmetric fixed points as well as three saddle points. The trajectories flowing toward the stable fixed points are separated by the separatrices.

Since the continuity equation implies that the probability at point $\vec{r}$ evolves according to $\vec{R}(t;\vec{r})$, we obtain a formal solution of Eq. (4):

$$p(\vec{n},t) = \int dxdy\, p(\vec{r},0)\,\delta^{(2)}(\vec{n}-\vec{R}(t;\vec{r})). \quad (5)$$

It implies that the initial probability distribution in the basin of attraction associated with a stable fixed point will eventually accumulate at that point. As a consequence, in the long time limit $t\to\infty$, the probability distribution becomes a sum of δ-function peaks at the stable fixed points denoted by $\vec{n}_i$:

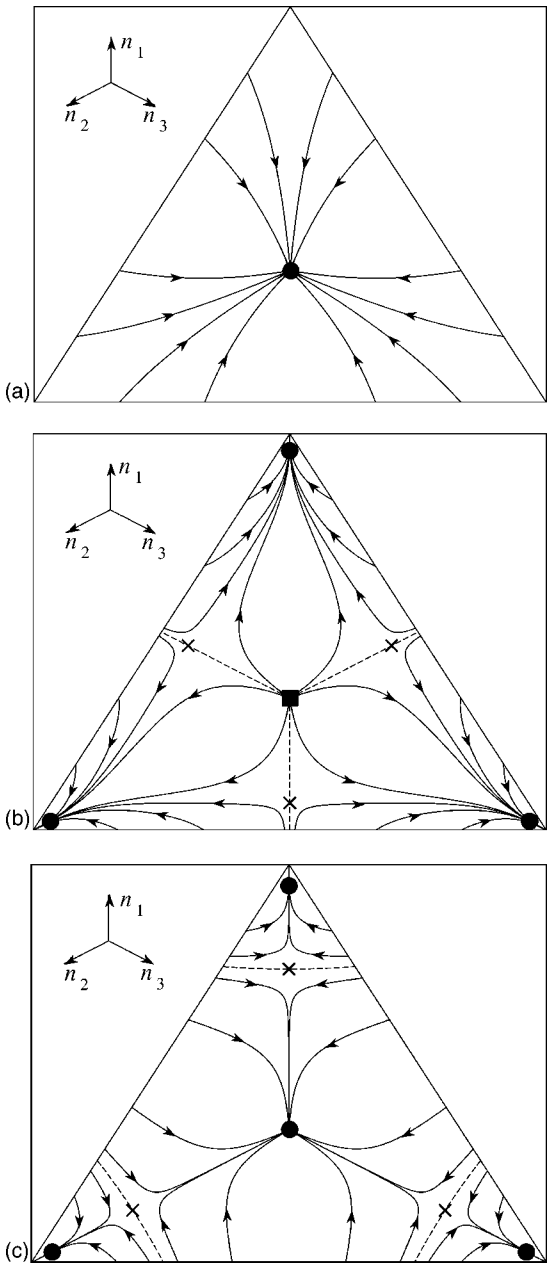

FIG. 2. Typical trajectories of Eq. (3). We plotted the trajectories in the diagonal plane of a unit cube so that each variable n_i is treated in the same way. (a) $\Delta=0.5$, $T_0=0.5$ (symmetric phase); (b) $\Delta=0.25$, $T_0=0.05$ (asymmetric phase); (c) $\Delta=1.0$, $T_0=0.1$ (mixed phase). The stable, the unstable, and the saddle point are represented with a filled circle, a filled square, and a cross, respectively.

$$p(\vec{n},\infty)=\sum_i p_i\delta^{(2)}(\vec{n}-\vec{n}_i), \tag{6}$$

where p_i are the sum of the initial probabilities in the basin of attraction associated with $\vec{n}_i$.

Now we consider another limit in the master equation (1), namely, we take the long time limit $t\to\infty$ before we take the limit $N\to\infty$. That is, we are looking for the stationary probability distribution for a finite system. Although this limit may not properly reflect the properties of the infinite system, we expect it will reveal interesting properties of the system concerning the characteristic times (see [10] in two-urn case).

Let us first take the long time limit of $t\to\infty$ in Eq. (1). In this limit we may drop off the time dependence in the probability distribution, which now takes the form

$$\begin{aligned}&\left[F\left(\frac{N_1+1}{N}\right)\frac{p(N_1+1,N_2-1,N_3)}{p(N_1,N_2,N_3)}-F\left(\frac{N_2}{N}\right)\right]\\&+\left[F\left(\frac{N_2+1}{N}\right)\frac{p(N_1,N_2+1,N_3-1)}{p(N_1,N_2,N_3)}-F\left(\frac{N_3}{N}\right)\right]\\&+\left[F\left(\frac{N_3+1}{N}\right)\frac{p(N_1-1,N_2,N_3+1)}{p(N_1,N_2,N_3)}-F\left(\frac{N_1}{N}\right)\right]\\&+\left[F\left(\frac{N_1+1}{N}\right)\frac{p(N_1+1,N_2,N_3-1)}{p(N_1,N_2,N_3)}-F\left(\frac{N_3}{N}\right)\right]\\&+\left[F\left(\frac{N_3+1}{N}\right)\frac{p(N_1,N_2-1,N_3+1)}{p(N_1,N_2,N_3)}-F\left(\frac{N_2}{N}\right)\right]\\&+\left[F\left(\frac{N_2+1}{N}\right)\frac{p(N_1-1,N_2+1,N_3)}{p(N_1,N_2,N_3)}-F\left(\frac{N_1}{N}\right)\right]=0.\end{aligned} \tag{7}$$

In contrast to the corresponding equation (13) in the two-urn model [10], it does not show a simple tridiagonal structure. However, we can show that the stationary probability distribution determined by Eq. (7) obeys the *detailed balance* [6]

$$F\left(\frac{N_i+1}{N}\right)p(N_1',N_2',N_3')=F\left(\frac{N_j}{N}\right)p(N_1,N_2,N_3), \tag{8}$$

where $\{i,j,k\}=\{1,2,3\}$ and $N_i'=N_i+1, N_j'=N_j-1$, $N_k'=N_k$. We also would like to note that this kind of relation is obeyed in the two-urn model. Equation (7) essentially tells us that the probability distribution for N_j is given by that for N_j-1, which is in turn given by that for N_j-2, and so on. Repeatedly using Eq. (7) with i as 1 or 2 and $i=3$, we obtain

$$p(N_1,N_2,N_3)=\frac{\prod_{k=1}^{N_1+N_2}F((N-k+1)/N)}{\prod_{i=1}^{N_1}F(i/N)\prod_{j=1}^{N_2}F(j/N)}p(0,0,N), \tag{9}$$

where $p(0,0,N)$ appears as an overall factor to normalize the probabilities so that we get

$$p(0,0,N)=\left[1+\sum_{N_1=0}^{N}\sum_{N_2=0}^{N-N_1}\frac{\prod_{k=1}^{N_1+N_2}F((N-k+1)/N)}{\prod_{i=1}^{N_1}F(i/N)\prod_{j=1}^{N_2}F(j/N)}\right]^{-1}.$$

Actually the urn model with fixed N belongs to the group of zero-range processes, so it is not surprising that Eqs. (8) and (9) can be read off straightforwardly from the results of zero-range processes (see [6]).

Now let us take the limit $N\to\infty$. With $N_1/N=n_1$, $N_2/N=n_2$, and scaling the probability distribution by N^2, the stationary probability distribution for large N now becomes

$$p(\vec{n}) \approx \frac{e^{NG(\vec{n})}}{\int_0^1 dx \int_0^{1-x} dy\, e^{NG(\vec{r})}}, \tag{10}$$

where

$$G(\vec{n}) = \int_0^{n_1+n_2} dt[\ln F(1-t)] - \int_0^{n_1} dt[\ln F(t)] - \int_0^{n_2} dt[\ln F(t)]. \tag{11}$$

We will call $G(\vec{n})$ the (negative) free energy function.

In the limit $N\to\infty$, the main contribution to the stationary probability distribution comes only from the maximum of $G(\cdot)$, and it becomes a sum of δ-function peaks. The maximum of $G(\vec{n})$ occurs when

$$\frac{\partial}{\partial n_1}G(\vec{n}) = \frac{\partial}{\partial n_2}G(\vec{n}) = 0 \tag{12}$$

or

$$F(n_1) = F(n_2) = F(n_3). \tag{13}$$

This condition is equivalent to the stationary condition of the flux equation (3). Note that in region II only three stable asymmetric solutions having the same maximum exist, while in region I only the symmetric solution is stable. Therefore the stationary probability distribution has triple peaks in region II and only the central peak in region I. In regions III and IV both the symmetric and the asymmetric solutions are stable so that the maximum of $G(\vec{n})$ should be determined by comparing its values at the stable fixed points. The crossover of the maximum point occurs when both values coincide. This implies that the transition between the triple peaks and the central single peak in the probability distribution is determined by the condition $\Delta G = G(\vec{n}_a) - G(1/3,1/3,1/3) = 0$, where $\vec{n}_a$ is one of the stable asymmetric fixed points. This condition yields a line that separates the two regions III and IV.

It is rather straightforward to extend our analytic results to the general case of many urns. For example, the free energy function for L urns is given by

$$G_L(\vec{n}) = \int_0^{1-n_L} dt\, \ln F(1-t) - \sum_{i=1}^{L-1} \int_0^{n_i} dt\, \ln F(t). \tag{14}$$

IV. CHARACTERISTIC TIME SCALE

One of the interesting phenomena in sands separated by compartments is the sudden collapse of a granular cluster [9,12]. It is observed experimentally that a granular cluster with the majority of sand grains in a single compartment remains stable for a long time until it collapses abruptly and diffuses over all compartments [12]. The urn model proposed in Ref. [9] displays the same phenomenon. In region I a granular cluster is stable up to a time scale τ, after which sand particles are distributed uniformly over all boxes. Approaching the phase boundary I-IV, the characteristic time scale diverges. At the phase boundary, it is found numerically that τ scales as $\tau\sim N^z$ with $z\simeq 0.32$ [9]. In this section, the scaling law for the characteristic time τ at and near the phase boundary is derived analytically.

The master equation in Eq. (4) in the large N limit does not contain a diffusive term. It implies that a δ-function-peaked probability distribution remains δ function peaked during time evolution, which enables us to write down the formal solution in Eq. (5). The dispersionless nature also guarantees that the mean-field approximation in Eq. (3) for the occupancy n_i becomes exact as long as the initial values of the n_i's are prescribed. Hence we can study the dynamics of the granular cluster using Eq. (3) with the initial conditions $n_1=n_2=0$ and $n_3=1$.

With $n_1=n_2=n$ and $n_3=1-2n$, one can rewrite Eq. (3) as

$$\dot{n} = V(n) \equiv \tfrac{1}{2}\{F(1-2n) - F(n)\} \tag{15}$$

with the initial condition $n(t=0)=0$. The cluster dynamics is then determined from the property of the flow function $V(n)$. In the inset of Fig. 1, we show the plots of the flow function at different values of T_0 with $\Delta=0.3$ fixed. At $\Delta=0.3$, the critical point separating the regions I and VI is given by $T_0=T_{0c}=0.1698\ldots$. For $T_0>T_{0c}$, $n=1/3$ is the unique stationary state solution; n grows from zero to $1/3$ to reach the symmetric state with $n_1=n_2=n_3=1/3$. Note that there exists a local minimum in $V(n)$ at $0<n_0<1/3$ where the flow velocity is minimum. Hence the value of n remains at the intermediate value $n\simeq n_0$ for a long time, and then converges to $n=1/3$ quickly. It turns out that the sudden collapse of a granular cluster [9,12] is due to the local minimum in $V(n)$. The characteristic time scale or the lifetime τ is given by

$$\tau = \int_0^{n_0} \frac{dn}{V(n)}. \tag{16}$$

As $T_0\to T_{0c}^+$, the minimum flow velocity $V(n_0)$ decreases and hence τ increases. The asymmetric solution with $n_1=n_2<n_3$ emerges at $T=T_{0c}$ when $V(n_0)=0$ and τ diverges.

The scaling law for the characteristic time scale is determined from the analytic property of $V(n)$ near $T_0\simeq T_{0c}$ and $n\simeq n_0$. One can expand as $V(n)\simeq a(n-n_0)^2+b(T_0-T_{0c})$, where a and b are constants of order 1 and all higher order terms in (T_0-T_{0c}) are irrelevant. Inserting it into Eq. (16), one obtains that the characteristic time scale diverges as $\tau\sim(T_0-T_{0c})^{-1/2}$ (see also Ref. [12]). At $T_0=T_{0c}$, the granular system approaches the asymmetric state algebraically in time as $|n-n_0|\sim t^{-1}$ whose lifetime τ diverges. That is to say, the asymmetric state is stable in the $N\to\infty$ limit.

However, for finite N, the system could evolve into the symmetric state at $T_0=T_{0c}$ with the help of statistical fluctuations in n. Indeed, the probability distribution p has a finite dispersion for finite N, even though it becomes a sum of δ-function peaks for infinite N. In order to estimate the order of magnitude of fluctuations in n, we investigate the station-

ary probability distribution in Eq. (10) at $T_0=T_{0c}$ in detail. Near the asymmetric state with $n_1=n_2=n$ and $n_3=1-2n$, the (negative) free energy function in Eq. (11) is written as $G(n)=\int_0^{2n}dt\ln F(1-t)-2\int_0^n dt\ln F(t)$. Now we expand it near $n=n_0$ to yield $G(n)=G(n_0)+G'(n_0)(n-n_0)+\frac{1}{2}G''(n_0)(n-n_0)^2+\frac{1}{3}G'''(n_0)(n-n_0)^3+\cdots$. After straightforward calculations, one can show that

$$G'(n_0) = 2\ln[F(1-2n_0)/F(n_0)], \tag{17}$$

$$G''(n_0) = \frac{2}{F(n_0)}V'(n_0), \tag{18}$$

$$G'''(n_0) = \frac{2}{F(n_0)}V''(n_0). \tag{19}$$

Note that $G'(n_0)=G''(n_0)=0$ since $V(n_0)=V'(n_0)=0$. Therefore, the (negative) free energy function can be approximated as $G(n)\simeq c(n-n_0)^3$ with a constant c, and hence the probability distribution as $p_s(n)\simeq e^{cN(n-n_0)^3}$ up to a normalization constant.

The stationary probability distribution suggests that the magnitude of the fluctuation in n near n_0 is of order $\delta n \sim N^{-1/3}$. With the help of the fluctuation, the granular system could get away from the asymmetric state when $|n(t)-n_0| \sim \delta n$, and flow into the symmetric state. Therefore the characteristic time scale is given by $\tau\simeq\int_0^{n_0-\delta n}dn/V(n)$, which results in $\tau\sim N^z$ with the dynamic exponent

$$z = 1/3. \tag{20}$$

Our analytic result confirms the numerical result $z\simeq 0.32$ reported in Ref. [9].

Note that the scaling behavior $\tau\sim N^{1/3}$ at the limit of stability is resulted from the fact that $V(n_0)=V'(n_0)=0$ and $V''(n_0)\neq 0$. The condition $V(n_0)=V'(n_0)=0$ amounts to the fact that the asymmetric states emerge as stable solutions, that is, the system is at the limit of stability. For generic expression of $T(n)$, $V''(n_0)$ is, in general, not zero, which results in the scaling behavior $\tau\sim N^{1/3}$. Therefore this scaling behavior is robust with respect to different forms of $T(n)$ or $F(n)$ [13].

V. CONCLUSIONS

We analytically investigate the three-urn model introduced by Coppex *et al.* [9] We formally solve the master equation of the model in the thermodynamic limit and find how the probability distribution evolves. In the long time limit, the probability distribution becomes δ-function peaks only at the stable fixed points. The strength of a δ-function peak is equal to the sum of initial probabilities in the basin of attraction associated with that fixed point.

We solve exactly the stationary probability distribution where we take the long time limit before we take thermodynamic limit. We find the distribution obeys the detailed balance. Regardless of the initial probability distribution it shows triple peaks or a single central peak depending on the parameters of the system. The final formula for the stationary probability distribution resembles that of equilibrium systems, where the transition from the triple peaks to the single peak is determined by the condition that the *free energies* of two phases become equal.

We also obtain the exact scaling law for the characteristic time scale τ which it takes to reach the symmetric state from an asymmetric state near and at the phase boundary I-VI. In the symmetric phase (region I), the granular cluster is unstable and τ is finite. It grows as one approaches the phase boundary as $\tau\sim(T_0-T_{0c})^{-1/2}$. At $T_0=T_{0c}$, the characteristic time diverges algebraically as $\tau\sim N^z$ with the dynamic exponent $z=1/3$. We also give a general argument that this scaling behavior is robust with respect to different expressions of the flux.

[1] L. P. Kadanoff, Rev. Mod. Phys. **71**, 435 (1999).
[2] H. J. Schlichting and V. Nordmeier, Math. Naturwiss. Unterr. **49**, 323 (1996).
[3] J. Eggers, Phys. Rev. Lett. **83**, 5322 (1999).
[4] A. Lipowski and M. Droz, Phys. Rev. E **65**, 031307 (2002).
[5] F. Spitzer, Adv. Math. **5**, 246 (1970).
[6] M. R. Evans, Braz. J. Phys. **30**, 42 (2000).
[7] S. Großkinsky, G. M. Schütz, and H. Spohn, J. Stat. Phys. **113**, 389 (2003).
[8] K. Jain and M. Barma, Phys. Rev. Lett. **91**, 135701 (2003).
[9] F. Coppex, M. Droz, and A. Lipowski, Phys. Rev. E **66**, 011305 (2002).
[10] G. M. Shim, B. Y. Park, and H. Lee, Phys. Rev. E **67**, 011301 (2003).
[11] I. Bena, F. Coppex, M. Droz, and A. Lipowski, Phys. Rev. Lett. **91**, 160602 (2003).
[12] D. van der Meer, K. van der Weele, and D. Lohse, Phys. Rev. Lett. **88** 174302 (2002).
[13] In general, the dynamic exponent is determined from the analytic property of the velocity function $V(n)$. When $d^kV/dn^k|_{n=n_0}=0$ for $k<\Delta$ and $d^\Delta V/dn^\Delta|_{n=n_0}\neq 0$, it is given by $z=(\Delta-1)/(\Delta+1)$.